ARMY RESEARCH LABORATORY

Design of the Transmission Electron Microscope (TEM) Sample Scriber Template as Developed to Improve and Simplify the Sample Preparation Procedure

by Wendy L. Sarney

ARL-TR-4299 **October 2007**

NOTICES

Disclaimers

The findings in this report are not to be construed as an official Department of the Army position unless so designated by other authorized documents.

Citation of manufacturer's or trade names does not constitute an official endorsement or approval of the use thereof.

Destroy this report when it is no longer needed. Do not return it to the originator.

Army Research Laboratory
Adelphi, MD 20783-1197

ARL-TR-4299 **October 2007**

Design of the Transmission Electron Microscope (TEM) Sampler Scriber Template as Developed to Improve and Simplify the Sample Preparation Procedure

Wendy L. Sarney
Sensors and Electron Devices Directorate, ARL

REPORT DOCUMENTATION PAGE

Form Approved
OMB No. 0704-0188

1. REPORT DATE *(DD-MM-YYYY)*	2. REPORT TYPE	3. DATES COVERED (From - To)
October 2007	Final	September 2005 to August 2007

4. TITLE AND SUBTITLE
Design of the Transmission Electron Microscope (TEM) Sampler Scriber Template as Developed to Improve and Simplify the Sample Preparation Procedure

5a. CONTRACT NUMBER

5b. GRANT NUMBER

5c. PROGRAM ELEMENT NUMBER

6. AUTHOR(S)
Wendy L. Sarney

5d. PROJECT NUMBER

5e. TASK NUMBER

5f. WORK UNIT NUMBER

7. PERFORMING ORGANIZATION NAME(S) AND ADDRESS(ES)
U.S. Army Research Laboratory
ATTN: AMSRDL-ARL-SE-EI
2800 Powder Mill Road
Adelphi, MD 20783-1128

8. PERFORMING ORGANIZATION REPORT NUMBER
ARL-TR-4299

9. SPONSORING/MONITORING AGENCY NAME(S) AND ADDRESS(ES)
U.S. Army Research Laboratory
2800 Powder Mill Road
Adelphi, MD 20783-1128

10. SPONSOR/MONITOR'S ACRONYM(S)

11. SPONSOR/MONITOR'S REPORT NUMBER(S)

12. DISTRIBUTION/AVAILABILITY STATEMENT
Approved for public release; distribution unlimited.

13. SUPPLEMENTARY NOTES

14. ABSTRACT
The image quality and visibility of the crystal planes in a TEM sample directly relate to how we initially cleave the wafer during the sample preparation process. For diffraction-contrast imaging, many defects and other crystalline features are orientation specific, and are only visible along certain zone axes. The resolution limits of the TEM dictate the preferred zone axes for phase-contrast imaging. The TEM Sample Scribing Template described here allows easy selection of the zone axes by cleaving the wafer along specific crystal directions.

15. SUBJECT TERMS
Transmission electron microscopy

16. Security Classification of:			17. LIMITATION OF ABSTRACT	18. NUMBER OF PAGES	19a. NAME OF RESPONSIBLE PERSON
a. REPORT	b. ABSTRACT	c. THIS PAGE			Wendy L. Sarney
U	U	U	U	28	19b. TELEPHONE NUMBER (*Include area code*) (301) 394-5761

Standard Form 298 (Rev. 8/98)
Prescribed by ANSI Std. Z39.18

Contents

List of Figures

List of Tables

INTENTIONALLY LEFT BLANK.

1. Introduction

The first preparation step for crystalline cross-sectional transmission electron microscope (TEM) samples requires sectioning and assembling a sample "sandwich". A prior technical report (*1*) describes this step along with the entire sample preparation procedure. The visibility of lattice planes and defects directly relates to the crystallographic direction of the electron beam with respect to the sample. The range of specimen tilt in the TEM is limited; therefore, how we initially cleave the wafer restricts which crystallographic directions are examinable.

Both TEMs at the U.S. Army Research Laboratory (ARL) have side-entry goniometer stages. The 2010 and 2010F TEMs currently have the high resolution and the analytical pole-piece installed, respectively. The pole-piece is a cylindrically symmetrical core of soft magnetic material with a hole drilled through it. The objective lens has a split pole-piece, meaning that there are two separate pole-pieces, each surrounded by a coil of copper wire. We insert the tip of the specimen rod into a very narrow gap located between the upper and lower pole-piece. This gap is especially small between the high-resolution pole pieces in the 2010 TEM. We are therefore limited in the extent that we can tilt the sample without touching the pole-piece. The allowed tilt range is ±12° in the x and y directions on the 2010 and ±27˚ in the x direction and ±15˚ in the y direction on the 2010F.

Regardless of the mechanical tilt limits, it is desirable to minimize the amount of tilting needed to examine a sample. Since the sample is approximately flat, positioning the sample so that the incident beam is normal to its surface minimizes the distance the beam must travel to penetrate the sample. As we tilt the sample, we gradually decrease the size of the electron transparent area (as the distance between a fixed point and the ion milled 'hole', as measured normal to the electron beam, decreases) and increase the specimen thickness along the beam direction. The extent of multiple diffraction increases with the distance the electron beam must travel to penetrate the sample. This leads to the appearance of diffraction spots that violate visibility conditions and makes interpreting the diffraction patterns difficult. Furthermore, the amount of averaged information in the final image increases with the sample thickness, leading to image artifacts that can be misleading or difficult to understand.

The lattice fringes seen in a high-resolution TEM image are dependent on the zone axis (*2*), which refers to the normal plane of the diffraction spot pattern. The zone axis is a common direction to all of the crystal planes corresponding to the spots in the diffraction pattern. Relative to the microscope itself, the sample's zone axis points in the direction of the electron gun. We choose our zone axis based on the details of the sample and the goals of the experiment.

For phase-contrast images, the best zone axis is usually the one that allows resolution of lattice fringes corresponding to more than one family of crystal planes. The $[1\,\bar{1}\,0]$ zone axis is

preferred for most high-resolution lattice imaging of the cubic semiconductor materials because imaging the $\{1\,\bar{1}\,0\}$ crystal face results in relatively easily resolvable {002} and {111} lattice fringes. In the case where the wafer has a (001) growth direction, the $[1\,\bar{1}\,0]$ zone axis is obtained by cleaving the sample parallel to the $(1\,\bar{1}0)$ plane. We scribe the sample perpendicular to the major flat with a diamond scribe and lightly tap the wafer until the small piece breaks free. Figure 1(b) shows the cleaved piece with its corresponding orientations. For the $[1\,\bar{1}\,0]$ zone axis, the sample is oriented in the TEM with the $(1\,\bar{1}0)$ face perpendicular to the electron beam. Figure 1(c) is a schematic of the diffraction pattern obtained, and figure 1(d) is a high-resolution image of GaSb examined along the $[1\,\bar{1}0]$ zone axis.

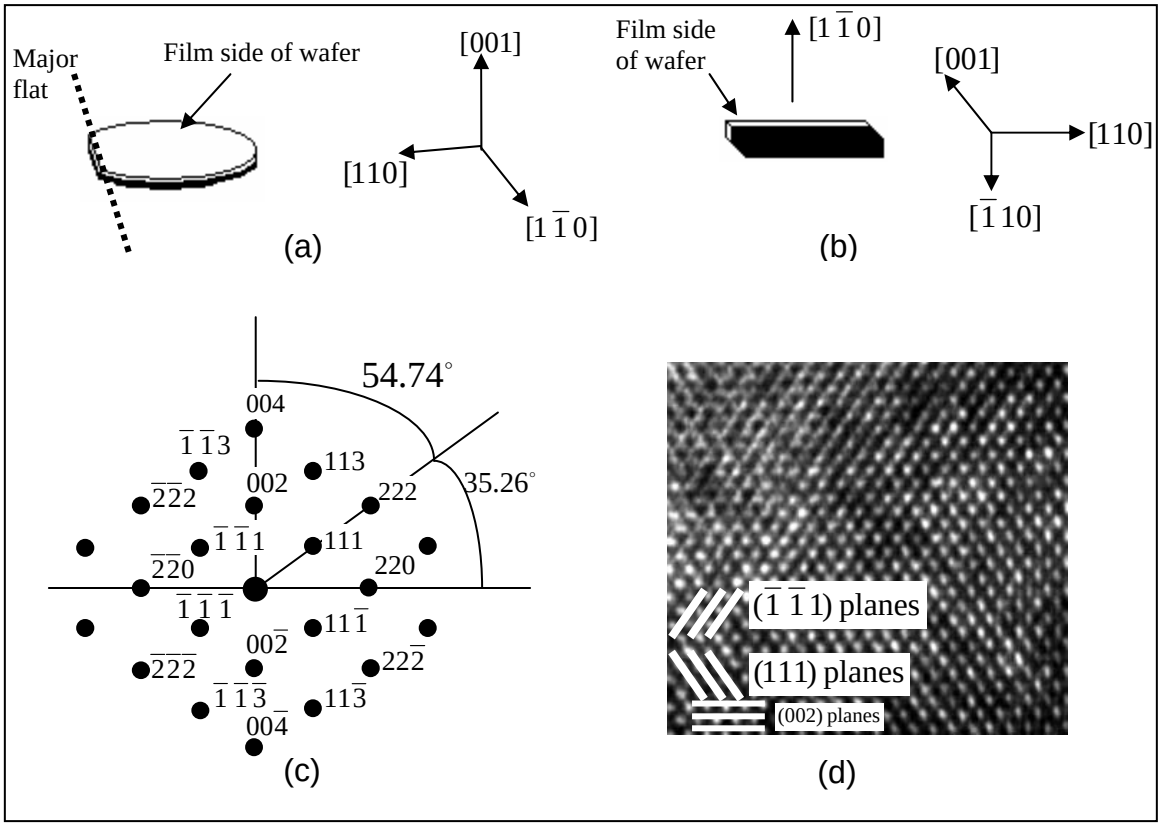

Figure 1. (a) Wafer with [001] growth direction. After scribing and cleaving the wafer along the dashed line the sample appears as shown in (b). The diffraction pattern (c) and high-resolution lattice image (d) resulting from a specimen examined as oriented in (b).

Occasionally the optimal image is not of the most easily resolved crystal planes and does not come from the sample most easily prepared. For example, AlGaAs/GaAs superlattices examined along the $[1\,\bar{1}\,0]$ zone axis show 'washed out' contrast between the very thin AlGaAs and GaAs layers washed out at high magnifications (*3*). The contrast improved when observed along the [100] zone axis, in agreement with experiments by Petroff (*4*) and Suzuki (*5*), et al. We obtain the [100] zone axis for a [001]-growth direction wafer by cleaving it 45˚ from the major flat, as

shown in figures 2a and 2b. The diffraction pattern obtained from examining a III-V cubic material along the [100] zone axis is shown schematically in figure 2(c).

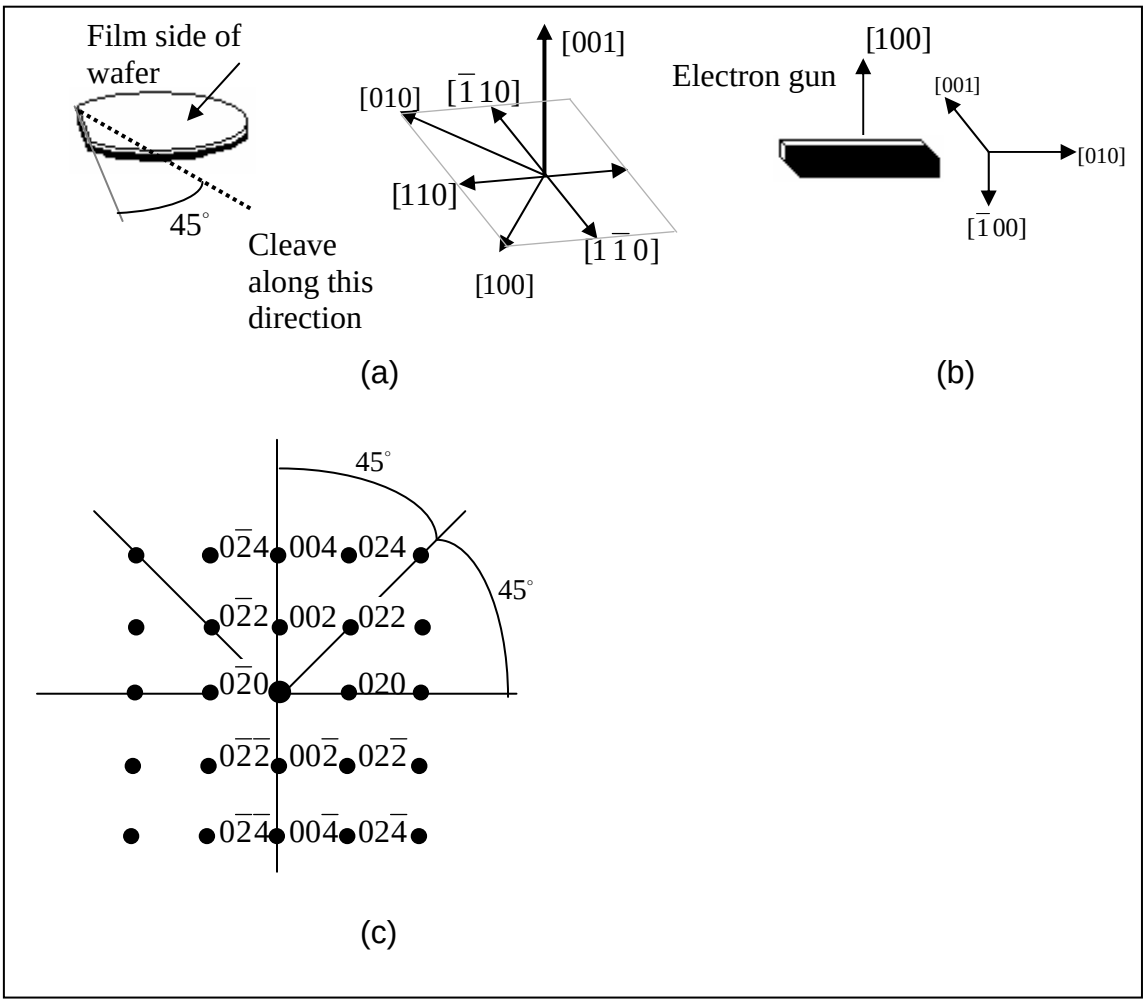

Figure 2. (a) Wafer with [001] growth direction. After scribing and cleaving the wafer along the dashed line the sample appears as shown in (b). The diffraction pattern (c) resulting from a specimen examined as oriented in (b).

When investigating the morphology of defects such as dislocations and stacking faults, we need to consider the visibility rules before selecting an appropriate zone axis. For instance, the invisibility criterion dictates that a dislocation will not be visible for , $\vec{g} \cdot \vec{b} = 0$ where $\vec{g}$ is the reciprocal lattice vector and $\vec{b}$ is the Burger's vector. As previously stated, each zone axis has a diffraction pattern containing spots that correspond to the reflecting planes in the specimen. We define the reciprocal lattice vectors $\vec{g}$ as those lying normal to the planes represented by the spots. When characterizing defects we often set up a two-beam condition, which involves slightly tilting the specimen away from the zone axis until only one diffracted beam is strong. We place an objective aperture around the excited beam and obtain a dark field image. The bright areas in the image meet the Bragg condition. By examining the same area under multiple

two-beam conditions, we can track the visibility of specific defects and determine their type. We prepare the sample with a zone axis that includes the diffraction spots that will allow the desired two-beam conditions.

Table 1 lists the strongest lattice fringes and lowest index diffraction spots corresponding to the most common zone axes in the cubic system. Using this information, we select the best zone axes for our sample based on the goals of the experiment. For instance, if x-ray data suggested that a film has defects of a certain type, we would select a zone axes that allow us to set up different two-beam conditions where the defect would be both visible and invisible.

Table 1. Zone axes and corresponding lattice fringes and diffraction spots.

Zone Axis	**Strongest Lattice Fringes Observed (for most materials)**	**Lowest Index Diffraction Spots**
$[1\,\bar{1}\,0]$	(111), (002), (220)	002, 111, 220, 113
[010]	(002), (200), (202)	002, 200, 202, 204
$[1\,\bar{1}1]$	(220), $(20\bar{2})$, $(0\bar{2}2)$	$[2\bar{2}0]$, $(20\bar{2})$, $(0\bar{2}2)$, $42\bar{2}$
$[11\bar{2}]$	(111), $[2\bar{2}0]$	111, $[2\bar{2}0]$, $3\bar{1}1$, 402
$[1\,\bar{1}\bar{3}]$	(220)	220, 301, $2\bar{4}2$, $4\bar{2}2$
$[02\,\bar{1}]$	(200)	200, $0\bar{2}\bar{4}$, , $4\bar{2}\bar{4}$
$[0\bar{3}1]$	(200)	200, 113, 026, 313
$[\bar{3}\bar{3}2]$	$[\bar{2}20]$	$\bar{2}20$, $\bar{1}\,\bar{1}\bar{3}$, $\bar{1}3\bar{3}$, $\bar{3}53$

The current 'state-of-the-art' procedure for the scribing process is to position a glass slide in a direction perpendicular to the zone axis and lightly scribe the wafer. When the desired zone axis is not parallel or perpendicular to the major flat, then one must determine the orientation of the preferred imaging plan relative to the flat, and then reposition the glass slide with the help of a protractor. Sample preparation is commonly delegated to graduate students or technicians who do not necessarily understand crystallography or reciprocal space. Browsing through technical publications with TEM images makes it clear that many samples have been prepared with the 'easiest' rather than the most appropriate zone axis.

Rather than using protractors and glass slides to scribe samples and to lift the burden of calculating angles between different crystallographic planes and directions, I have designed a set of TEM Sample Scribing Templates. The preferred embodiment of this set of tools allows the user to quickly and easily determine where the sample must be scribed in order to obtain the desired zone axis. This saves time, reduces mistakes, and improves sample quality and therefore encourages the user to prepare the most appropriate sample for their particular experiment.

2. Design of the TEM Sample Scribing Templates

The system consists of five templates and one T-square. The tools can be made of any material that is resilient to the solvents (acetone and methanol) typically present in a TEM sample preparation lab. We constructed our tools with aluminum. The crystal structure of the films examined by our division is usually cubic and occasionally hexagonal. The III-V cubic materials (such as the GaAs based structures) are usually grown on [001] growth-oriented substrates and occasionally grown on [111]-oriented substrates. The II-VI cubic materials (such as CdTe) are grown on [001], [111], [211], and [311] growth-oriented substrates with [211] Si being the most common choice. The hexagonal films (usually GaN-based structures) have the [0001] growth direction. We designed 5 templates that are used for cubic wafers having the [001], [111], [211], and [311] growth directions and hexagonal wafers having the [0001] growth direction. These five templates allow us to cleave samples with the most common zone axes for all of our current projects. It is possible to add templates that are appropriate for other crystal structures (such as rhombohedral or orthorhombic.) and/or growth directions if the need arises.

Figure 3 is a schematic of the Scribing Template for cubic films with a [001] growth direction. The tool consists of a regular hexagonal prism cut from an aluminum rectangular prism having dimensions of 5 cm x 5 cm x 0.4 cm. Figure 3 consists of the (a) top and (b-c) two side views labeled with the dimensions that correspond to our prototype tools. The dimensions best accommodate the size of the wafers typically studied at ARL, however, there are no strict size requirements so long as the tool is easy to handle. Figure 3(d) shows the top view labeled with the zone axes obtained by lining the T-square along each edge of the hexagon.

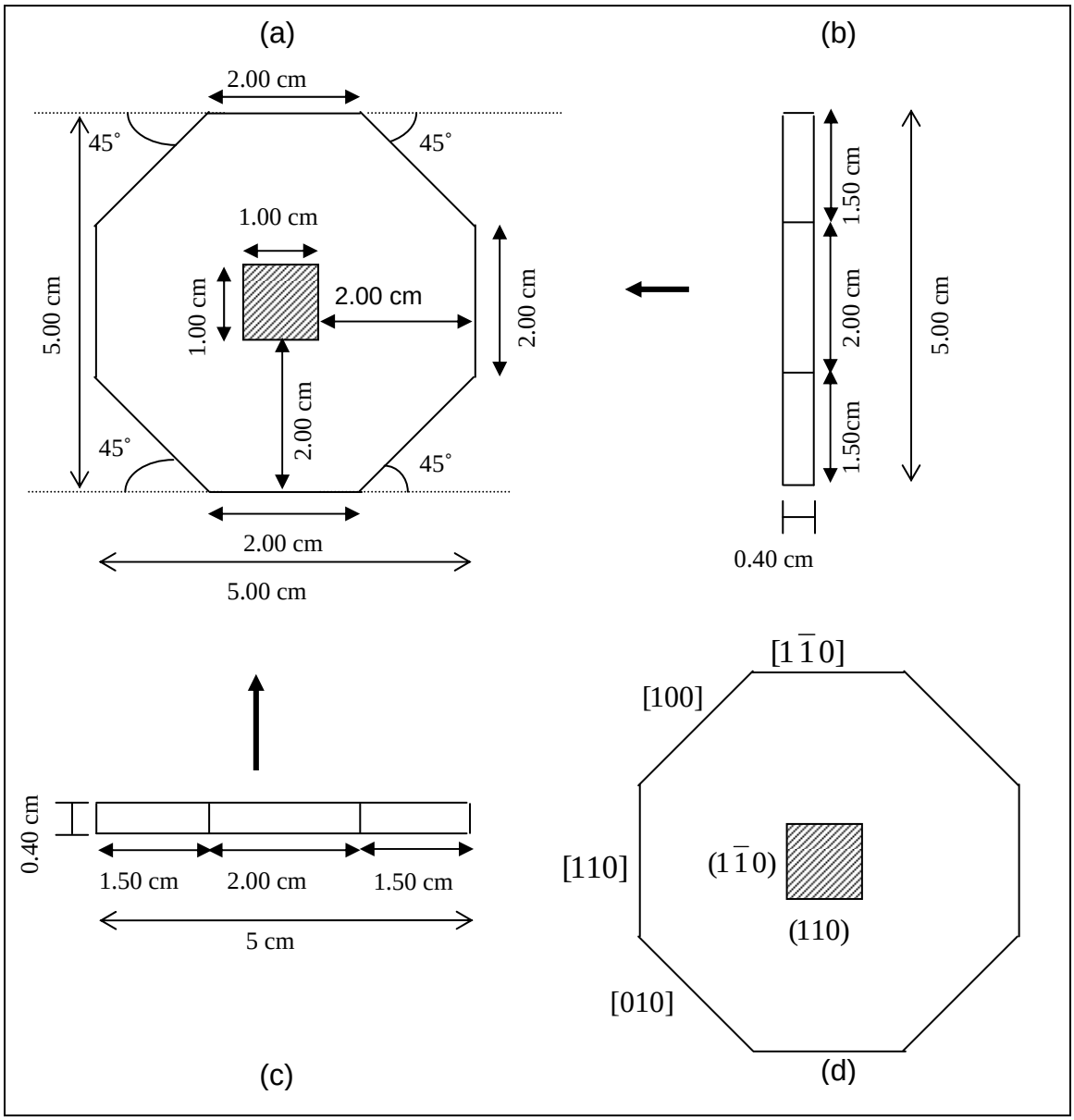

Figure 3. Sematics of Scribing Template for cubic materials with the [001] growth direction. Top (a) and side (b) and (c) views with labeled dimensions. Top (d) view with labeled orientations.

Figure 4(a) shows an uncleaved wafer, film side up, having a [001] growth direction and a (110) major flat. Ordinarily we receive a small portion of the wafer, usually a semicircle, square, or rectangle having dimensions on the order or 0.5 cm – 1.5 cm (as shown schematically by the region outlined by the crosshatched line in figure 4a). Figures 4(b)-(c) show the crystallographic orientations of the film side up and film side down wafer pieces. The sample is mounted film-side down onto the center of the template in the area marked with the hatched square (figure 4d). Ideally, the tool would be constructed so that the area represented by the hatched square was slightly recessed, so that the sample would not slip. In our current embodiment, the center square area is drawn on and used simply as a guide for positioning the sample. We align the

major flat with the bottom edge of the hatched square. We position the short edge of the T-square along the hexagon edge labeled with the desired zone axis. Figure 4(e) shows the T-square edge positioned against the $[1\bar{1}0]$ labeled hexagon edge. We place the T-square over the substrate side of the specimen so that its long edge is parallel to and located approximately 1.5 mm away from the $(1\bar{1}0)$ plane of the sample. A diamond scriber is drawn over the substrate side of the sample along the long edge of the T-square. The scribed line is parallel to the [110] direction in the film, and perpendicular to the $[1\bar{1}0]$ direction. We then cleave the sample by compressing the wafer with two glass slides and lightly tapping on the cleaved edge with the blunt side of a pair of tweezers. Since our sample sandwich requires rectangular pieces we scribe the cleaved piece perpendicular to the initial scribed line to obtain the desired size (approximate size is 1.5 x 4 mm). Figure 4f shows the cleaved piece labeled with its corresponding crystallographic directions.

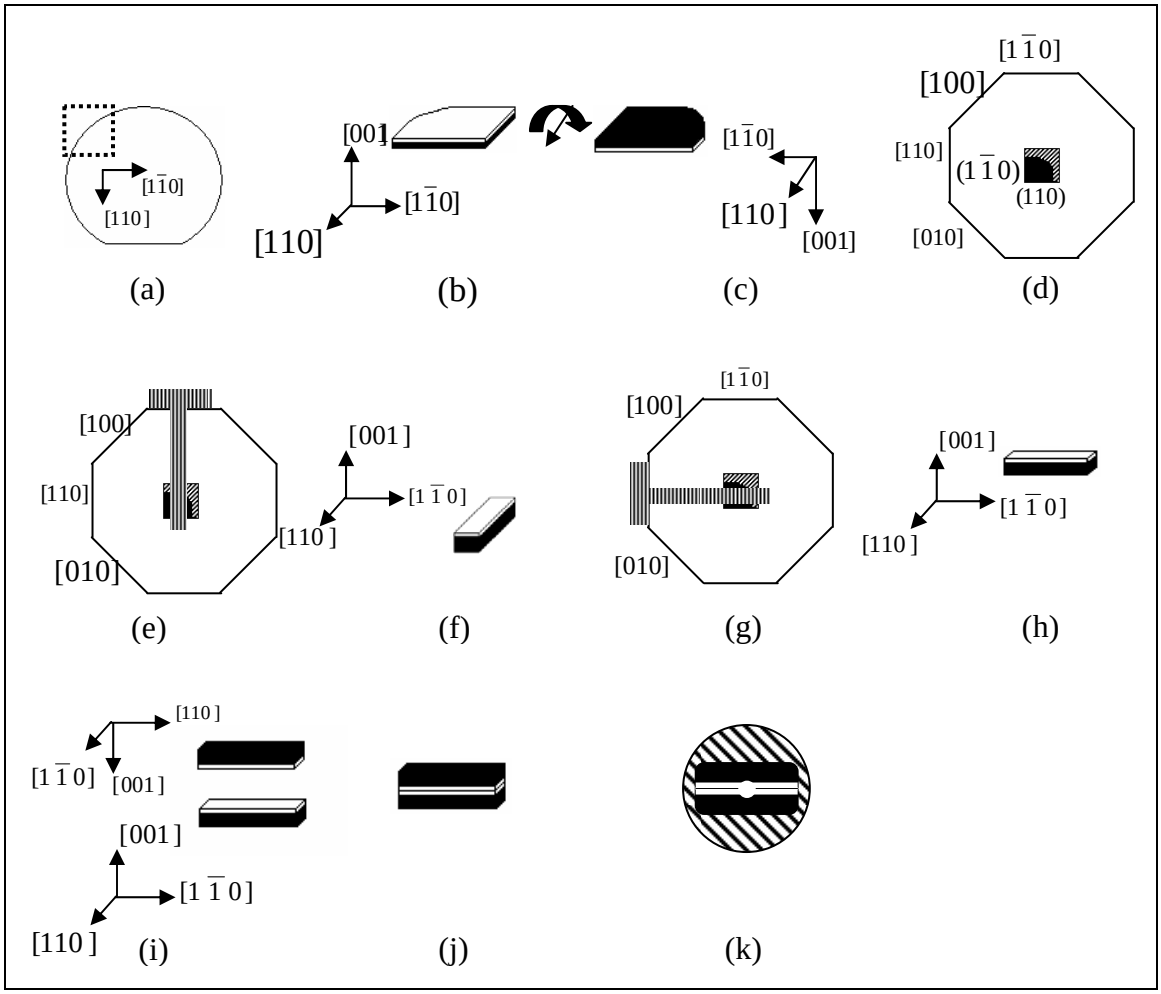

Figure 4. Scribing process for a film having a (001) growth direction and a (110) major flat. (a) The initial wafer, (b) a piece as typically received by the grower (also denoted by the hatched square in (a)), (c) the crystallographic directions of the piece after it is rotated so that the film side faces downward. (d) The scribing template for III-V films having a (001) growth direction. (e) The T-square is placed so that a sample having a [110] zone axis is obtained. (f) The cleaved piece and its corresponding crystallographic orientations. (g) T-square arranged to scribe a sample with a [110] zone axis. (h) The cleaved piece and its corresponding crystallographic orientations and (i) the crystallographic relationship of the two cleaved pieces. (j) The sample after the two pieces are 'sandwiched' together with epoxy, (k) the thinned sample mounted on a 5 mm copper grid.

We need a second small piece to complete our sandwich structure, and we typically scribe and cleave it at a 90˚ orientation relative to the first piece. The T-square is oriented as shown in figure 4g and the resulting cleaved piece is oriented as shown in figure 4h. Figure 4i shows the arrangement of the two pieces before they are sandwiched together as shown in figure 4j. The sample is thinned, mounted onto a copper grid, and ion milled to electron transparency (figure 4k). The ion-milled hole crosses both pieces of the sandwich. Therefore, the upper piece of the sandwich can be examined along the $[1\,\bar{1}0]$ zone axis and the lower piece can be examined along

the [110] zone axis. This allows a more thorough characterization of the specimen, especially in the cases of certain orientation-dependent structures such as quantum wires (*1*).

In the case of certain superlattices, as discussed previously in this report for AlGaAs/GaAs structures, it is desirable to examine the sample along the [100] zone axis. In these situations, we arrange the T-square as shown in figure 5a and scribe two parallel lines oriented 45˚ from the major flat. The resulting piece (figure 5b) is usually sandwiched with a second piece having a [010] zone axis or a [110]-type zone axis.

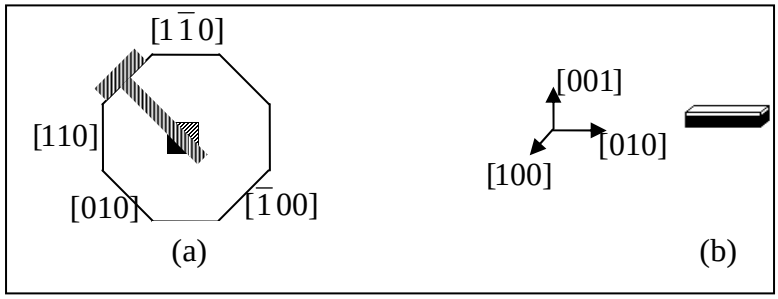

Figure 5. (a) T-square oriented to obtain a sample with a [100] zone axis and [001] growth direction. (b) The crystallographic orientations of the cleaved piece.

Figures 6 through 8 are schematics of the scribing templates for cubic materials with the [111], [211], and [311] growth directions, respectively. As in figure 3, each schematic has top and two side views with the dimensions of our prototype tools and a top view labeled with the most frequently desired zone axes. Figure 9 is a similar schematic of a template designed for use with hexagonal materials having a [0001] growth direction. Figure 10 shows the (a) top and (b-c) side views of the T-square. Figure 11 shows a photograph of the scribing template for the [211] growth direction and the T-square.

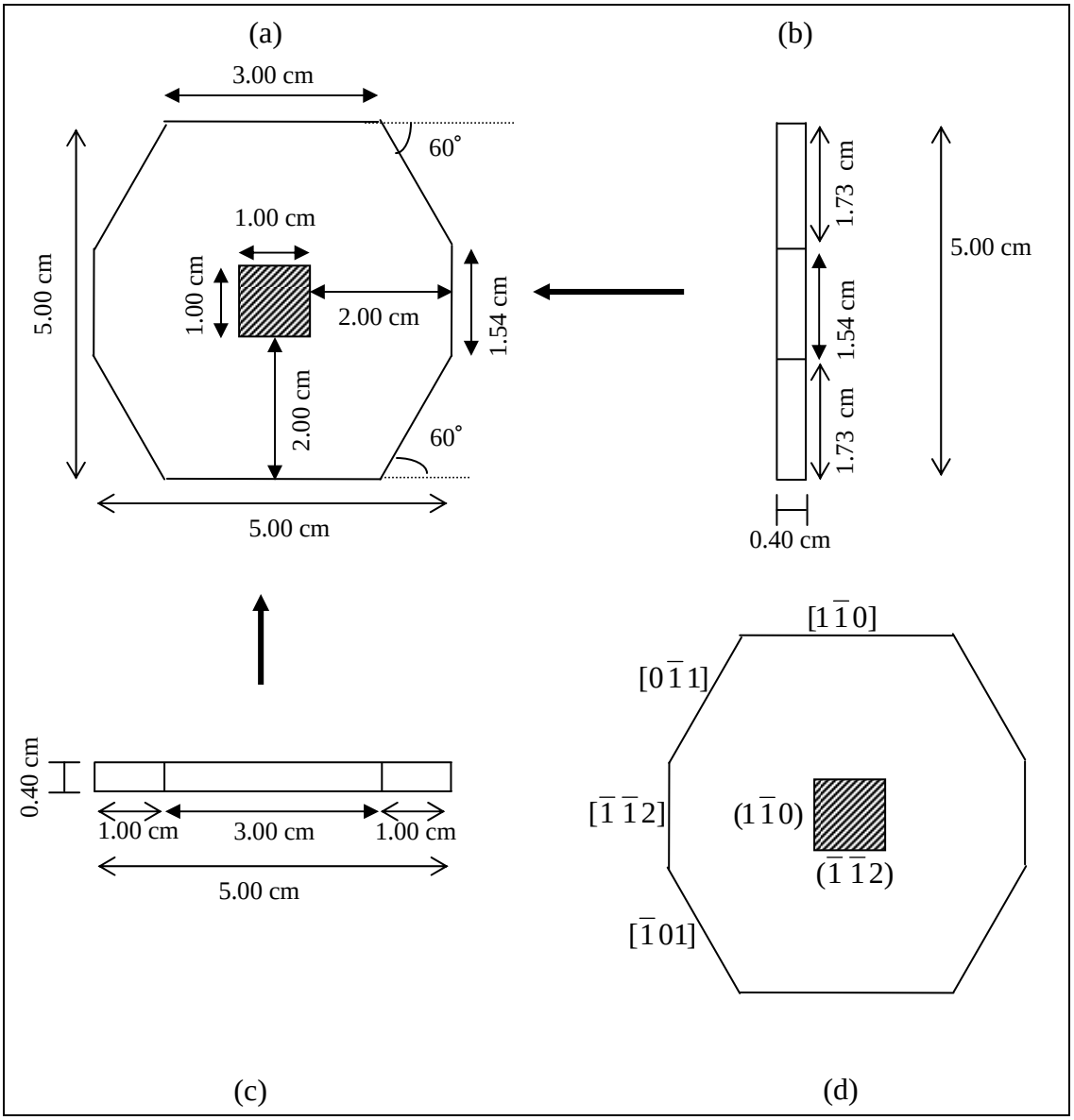

Figure 6. Schematics of Scribing Template for cubic materials with the [111] growth direction. Top (a) and side (b) and (c) views with labeled dimensions. Top (d) view with labeled orientations.

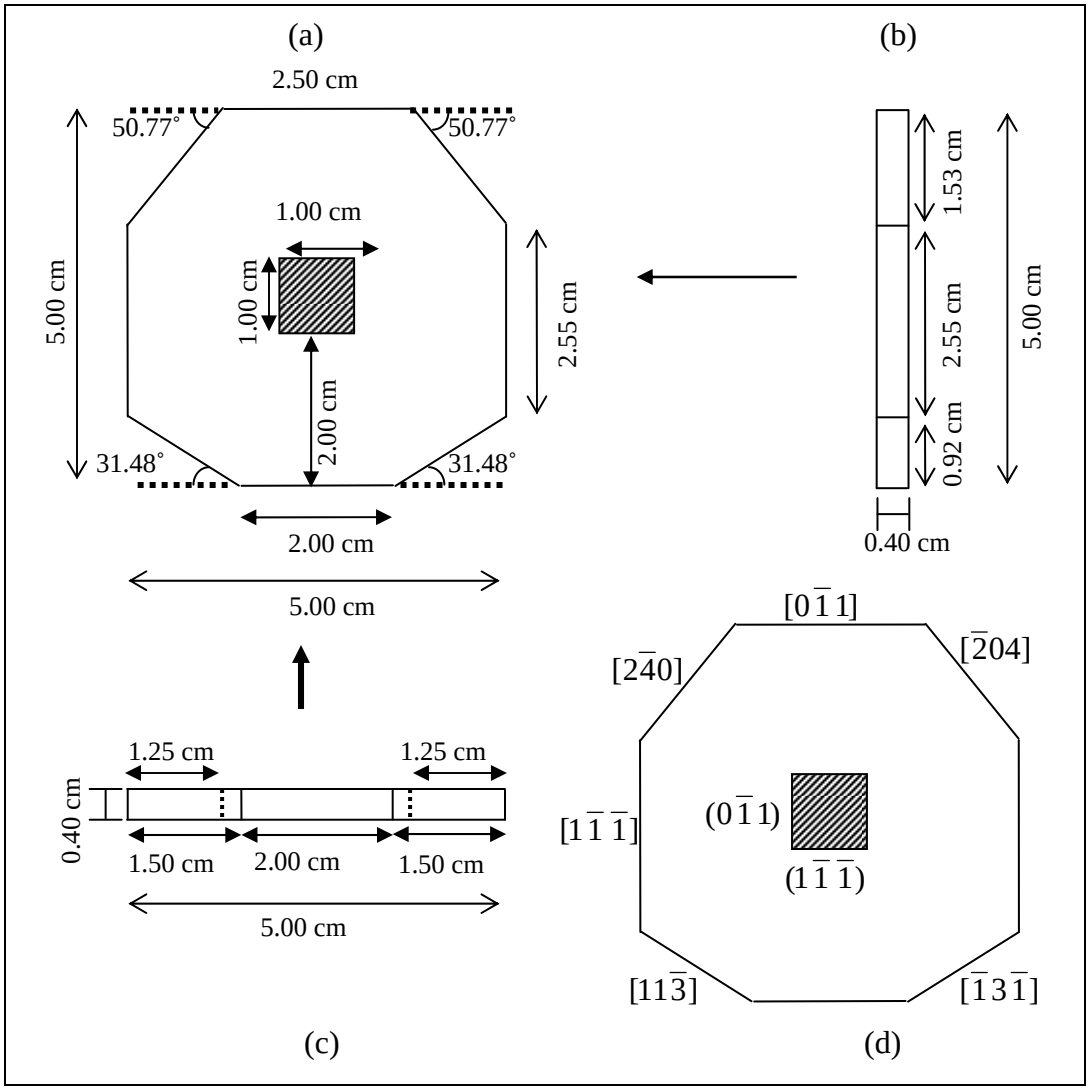

Figure 7. Schematics of Scribing Template for cubic materials with the [211] growth direction. Top (a) and side (b) and (c) views with labeled dimensions. Top (d) view with labeled orientations.

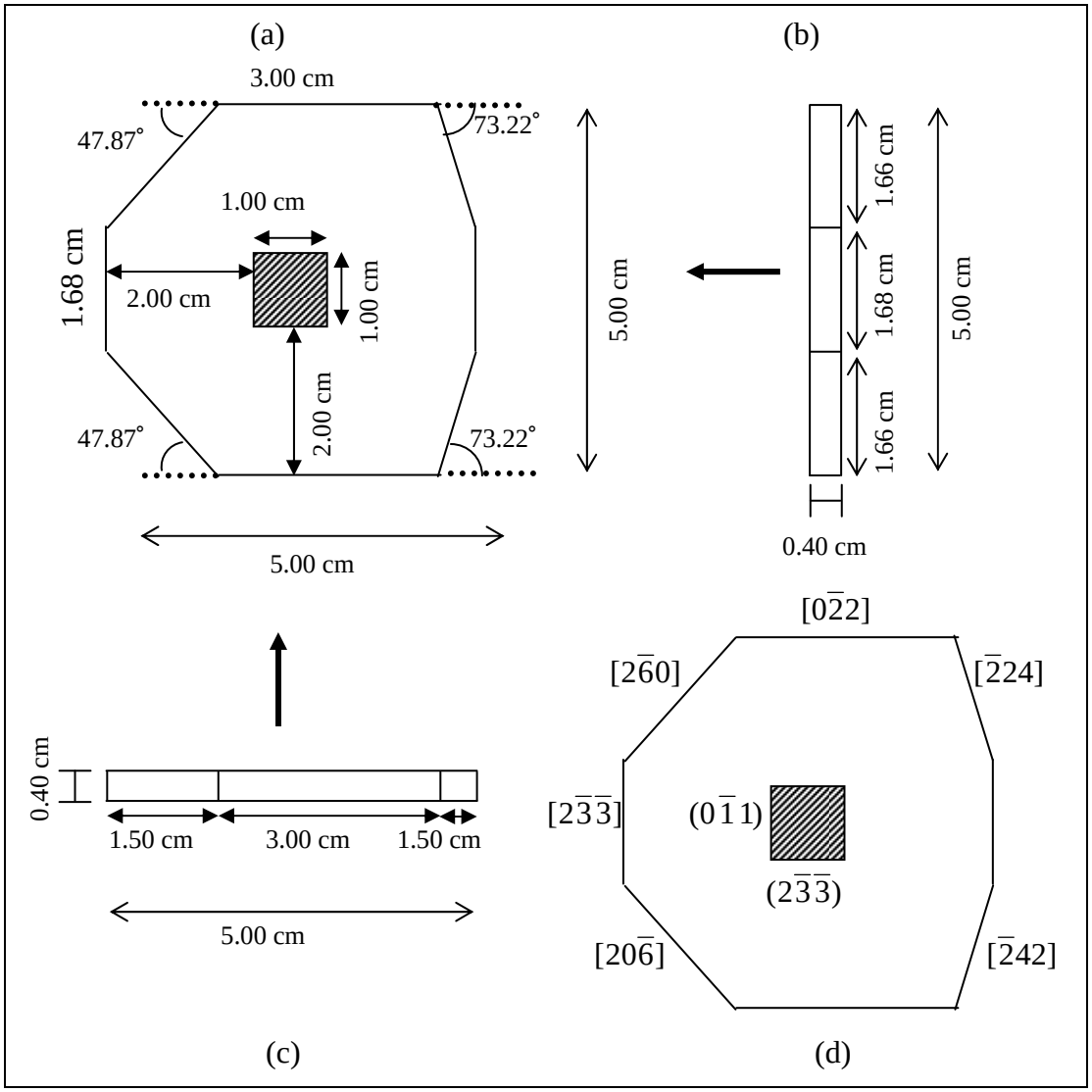

Figure 8. Schematics of Scribing Template for cubic materials with the [311] growth direction. Top (a) and side (b) and (c) views with labeled dimensions. Top (d) view with labeled orientations.

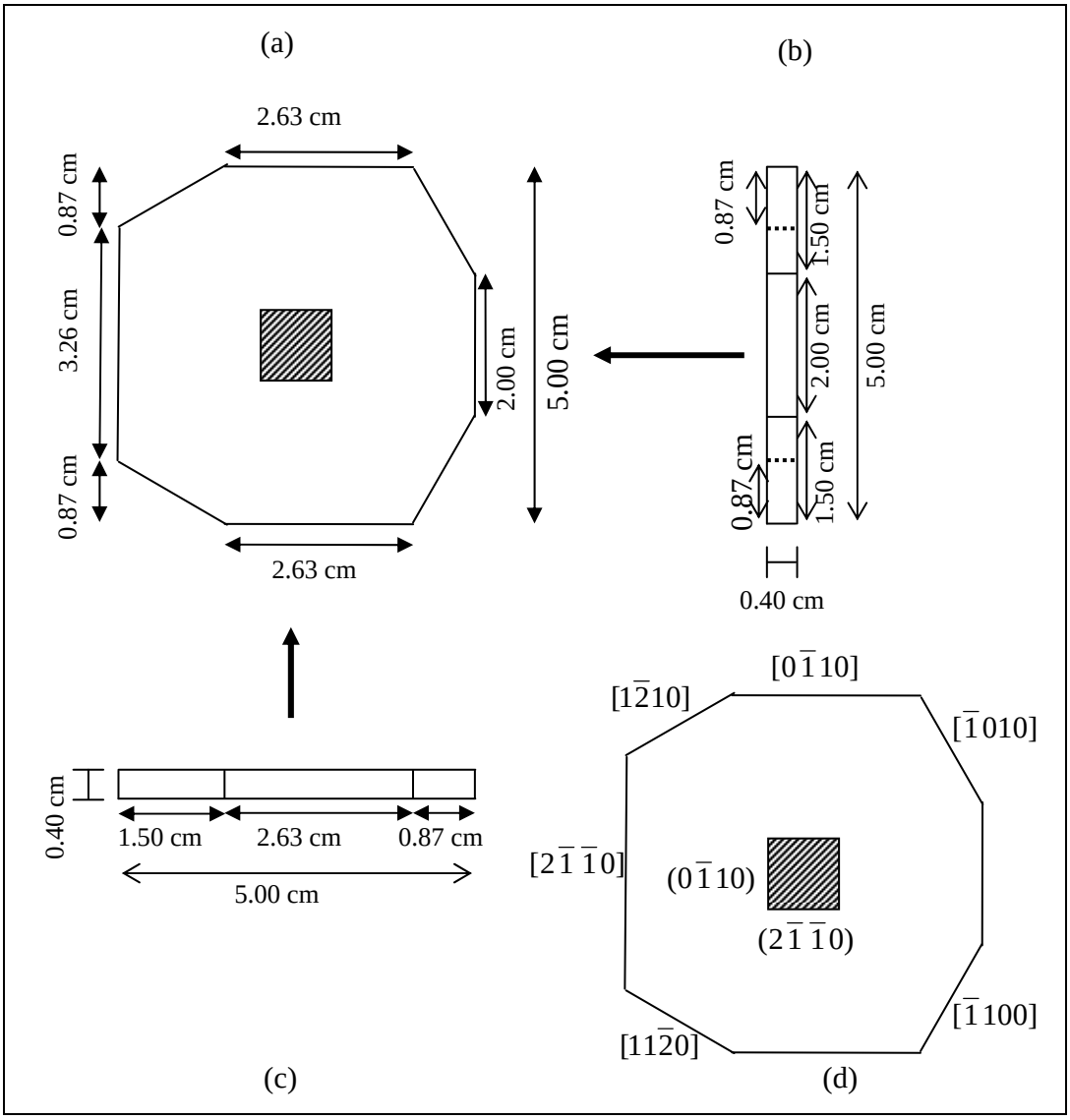

Figure 9. Schematics of Scribing Template for hexagonal materials with the [0001] growth direction. Top (a) and side (b) and (c) views with labeled dimensions. Top (d) view with labeled orientations.

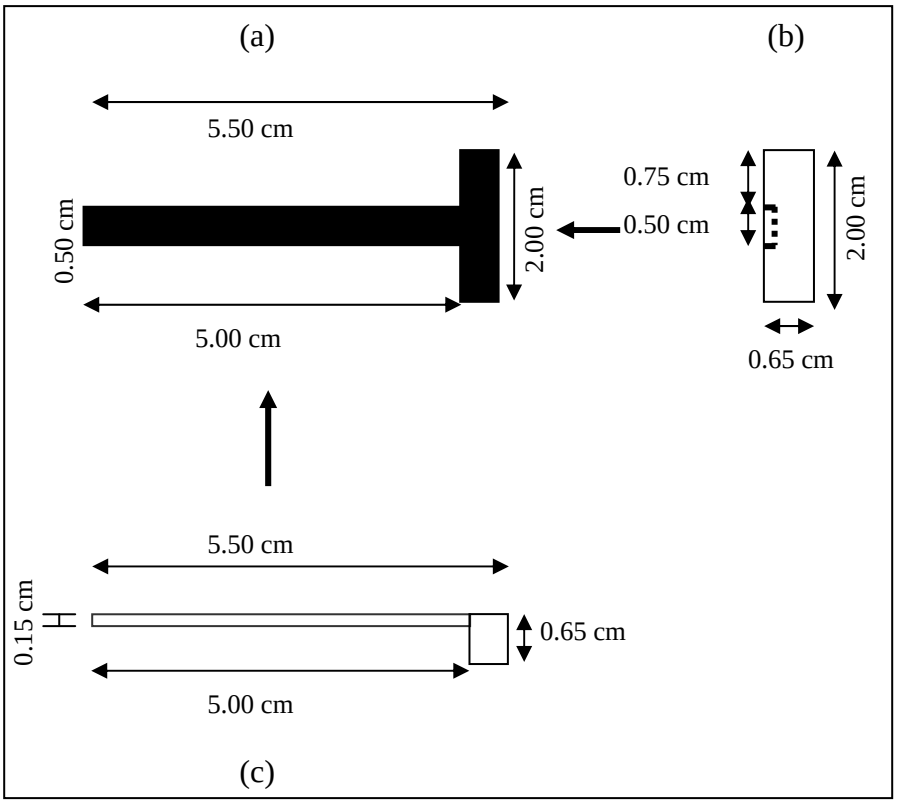

Figure 10. Top (a) and side (b) and (c) schematics of the T-square for the Scribing Template.

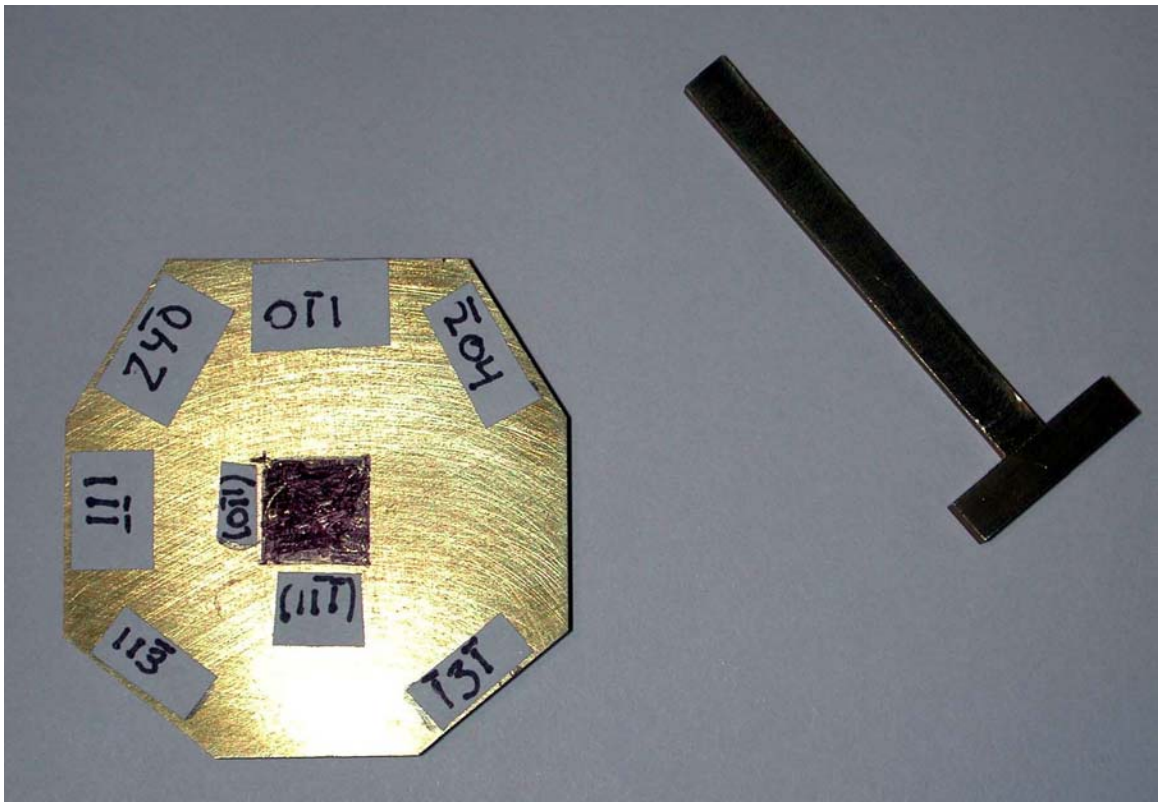

Figure 11. Photograph of the Scribing Template for the [211] growth direction and the T-square.

Some samples, such as GaN films grown onto SiC, are too hard to cleave with a diamond scriber. In this case, we use the tool with the diamond scriber to scribe a line with the desired orientation, and then move the sample to a diamond saw. Some commercially available diamond wire saws use a square graphite mount for positioning the samples. Adjusting the dimensions of the scribing template would allow the design of a tool that would fit directly into the wire saw.

Most of the films grown at ARL have the same in and out-of-plane orientations as the substrates onto which they are grown. In cases where the film and substrate do not have the same orientation, one must remember that using the tool as described in this report results in a sample having the zone axis selected by the T-square placement for the substrate only. For known in-plane misorientations (such as the 30˚ in-plane rotation between GaN and SiC), the sample can be rotated before placement onto the tool in a manner that allows us to select the zone axis for the film. In another example, we have studied ZnTe films with [111] growth direction grown onto Si substrates with a [311] growth direction. Since quality of the film image is usually more important than the substrate image, we choose the tool that corresponds to the growth direction of the film. In the ZnTe[111]/Si[311] system the $[1\,\bar{1}0]$ in-plane direction in the substrate does correspond to the $[1\,\bar{1}0]$ direction in the film, we can align the major flat of the wafer onto the template in the normal manner.

3. Conclusion

We use the sample scriber templates in the first step towards preparing TEM samples with the most appropriate zone axis for the experiment. The template's design allows fast selection amongst the most common zone axes for high- and low-resolution imaging. The system of templates is easily expandable to accommodate other crystal geometries.

4. References

1. Sarney, Wendy L. *Sample Preparation Procedure for TEM Imaging of Semiconductor Materials*; ARL-TR-3223; U.S. Army Research Laboratory: Adelphi, MD, 2004.

2. Sarney, Wendy L. *Understanding Transmission Electron Microscopy Diffraction Patterns Obtained From Infrared Semiconductor Materials*; ARL-TR-3128; U.S. Army Research Laboratory: Adelphi, MD, 2003.

3. Tobin, M. S.; Bruno, J. D. Quantum-confined stark effect modulator based on multiple triple-quantum wells. *Journal of Applied Physics* **2001**, *89* (3), 1885–1889.

4. Petroff, P. M. Transmission electron microscopy of interfaces in III-V compound semiconductors. *J. Vac. Sci. Technol.* **1977**, *14* (4) 973–978.

5. Suzuki, Y; Okamoto, H. Transmission electron microscope observation of lattice image of $Al_xGa_{1-x}As$-$Al_yGa_{1-y}As$ superlattices with high contrast. *J. Appl. Phys* **1985**, *58* (9), 3456–3462.

INTENTIONALLY LEFT BLANK

Distribution List

ADMNSTR
DEFNS TECHL INFO CTR
ATTN DTIC-OCP (ELECTRONIC COPY)
8725 JOHN J KINGMAN RD STE 0944
FT BELVOIR VA 22060-6218

DARPA
ATTN IXO S WELBY
3701 N FAIRFAX DR
ARLINGTON VA 22203-1714

OFC OF THE SECY OF DEFNS
ATTN ODDRE (R&AT)
THE PENTAGON
WASHINGTON DC 20301-3080

US ARMY TRADOC
BATTLE LAB INTEGRATION & TECHL DIRCTRT
ATTN ATCD-B
10 WHISTLER LANE
FT MONROE VA 23651-5850

SMC/GPA
2420 VELA WAY STE 1866
EL SEGUNDO CA 90245-4659

US ARMY INFO SYS ENGRG CMND
ATTN AMSEL-IE-TD F JENIA
FT HUACHUCA AZ 85613-5300

COMMANDER
US ARMY RDECOM
ATTN AMSRD-AMR W C MCCORKLE
5400 FOWLER RD
REDSTONE ARSENAL AL 35898-5000

US ARMY RSRCH LAB
ATTN AMSRD-ARL-CI-OK-TP TECHL LIB T LANDFRIED
BLDG 4600
ABERDEEN PROVING GROUND MD 21005-5066

US GOVERNMENT PRINT OFF
DEPOSITORY RECEIVING SECTION
ATTN MAIL STOP IDAD J TATE
732 NORTH CAPITOL ST., NW
WASHINGTON DC 20402

DIRECTOR
US ARMY RSRCH LAB
ATTN AMSRD-ARL-RO-EV W D BACH
PO BOX 12211
RESEARCH TRIANGLE PARK NC 27709

US ARMY RSRCH LAB
ATTN AMSRD-ARL-CI-OK-T TECHL PUB (2 COPIES)
ATTN AMSRD-ARL-CI-OK-TL TECHL LIB (2 COPIES)
ATTN AMSRD-ARL-D J M MILLER
ATTN AMSRD-ARL-SE-E G WOOD
ATTN AMSRD-ARL-SE-E H POLLEHN
ATTN AMSRD-ARL-SE-EI D BEEKMAN
ATTN AMSRD-ARL-SE-EI W SARNEY (20 COPIES)
ATTN AMSRD-ARL-SE-EM G SIMONIS
ATTN IMNE-ALC-IMS MAIL & RECORDS MGMT
ADELPHI MD 20783-1197

INTENTIONALLY LEFT BLANK